BUBBLE BEHAVIOR IN LIQUIDS CONTAINED IN VERTICALLY VIBRATED TANKS

BY

DANIEL D. KANA
FRANKLIN T. DODGE

TECHNICAL REPORT NO. 4
CONTRACT NO. NAS8-11045
CONTROL NO. TP3-85175 & S-1 (IF)
SwRI PROJECT NO. 02-1391

PREPARED FOR

NATIONAL AERONAUTICS AND SPACE ADMINISTRATION
GEORGE C. MARSHALL SPACE FLIGHT CENTER
HUNTSVILLE, ALABAMA

1 AUGUST 1964

SOUTHWEST RESEARCH INSTITUTE
SAN ANTONIO HOUSTON

SOUTHWEST RESEARCH INSTITUTE
8500 Culebra Road, San Antonio, Texas 78206

BUBBLE BEHAVIOR IN LIQUIDS CONTAINED IN VERTICALLY VIBRATED TANKS

by

Daniel D. Kana
Franklin T. Dodge

Technical Report No. 4
Contract No. NAS8-11045
Control No. TP3-85175 & S-1 (1F)
SwRI Project No. 02-1391

Prepared for

National Aeronautics and Space Administration
George C. Marshall Space Flight Center
Huntsville, Alabama

1 August 1964

APPROVED:

H. Norman Abramson, Director
Department of Mechanical Sciences

ABSTRACT

33511

Violent bubble behavior observed in liquids contained in a vertically vibrating tank is analyzed both theoretically and experimentally. The behavior is characterized by the occurrence of bubble motions that are contrary to usual buoyancy conditions, and of a pressure resonance well below the resonant frequency of a pure liquid column. It is found that the most violent part of the behavior is a result of a water hammer pressure resonance in a bubbly liquid-air mixture contained in an elastic tank. The theory set forth explains the entire behavior quite satisfactorily as evidenced by good agreement between the theory and experiments for the conditions studied.

TABLE OF CONTENTS

LIST OF FIGURES

INTRODUCTION

A number of investigators have observed that small vapor bubbles entrained in a column of liquid which is vibrated in a vertical direction do not always rise and vent from the liquid, but in some cases will remain suspended, migrate toward the walls of the container, or even sink to the container bottom. Such behavior of gas bubbles in liquids subjected to vibration has become of increasing interest because of its possible application to liquid fuel rockets and space vehicles. The occurrence of gas bubbles in liquid propellants can have detrimental effects on the performance of high speed turbine pumps, and therefore on the overall performance of a vehicle. Since intense vibrational conditions exist during various phases of the launch and flight of most vehicles, it immediately becomes necessary to determine whether these conditions are capable of producing the undesirable bubble behavior. The purpose of the present study is to obtain a better understanding of such bubble behavior in order to help make this determination.

Basically, the present work involves a preliminary experimental study conducted to observe the qualitative aspects of the bubble behavior, the development of a theory to explain the behavior and subsequent experimental studies conducted to obtain data to correlate with the developed analysis. A review of previous studies of bubble motion in vertically

vibrated liquids has been conducted and reported in [1]; therefore, a summary of all of those studies will not be presented here. However, since the analysis of the present work is essentially a modification of the theory developed by Bleich [2], his work will be discussed in some detail.

PRELIMINARY EXPERIMENTS

Previous investigators [2, 3, 4] have observed various bubble motions in liquids in vertically vibrated tanks, and have advanced a few theoretical analyses aimed at explaining the behavior. Although qualitative prediction of some of the observed behavior was accomplished, quantitative correlation of experiments with the theory was not good.

Preliminary experiments were conducted in the present study to observe qualitatively the various bubble motions that occur in vertically vibrated tanks, and to get preliminary data which would either tend to support the previously developed theories, or indicate the necessity of developing a new theory. These experiments were conducted primarily in a 24.13 cm (9-1/2 inch) diameter, 0.635 cm (1/4 inch) wall, 99.1 cm (39 inch) high, transparent acrylic plastic circular cylindrical tank, having a thick flat aluminum bottom. The preliminary observations were performed by visually observing bubble behavior in a 76.2 cm (30 inch) column of water in the tank, while it was vibrated at various accelerations on a mechanical shake table. Because of the shake table design, frequency was limited to 55 cps or less and table displacement amplitude to 0.152 cm (0.060 inch) or less.

A variety of complicated bubble behavior was observed in these experiments, depending on the vibrational input conditions. However, for the sake of brevity, the overall behavior will be summarized with the aid

of Figures 1 through 4, as it was observed to occur in the case of fixed input condition of 7 g's acceleration at about 45 cps frequency*.

The onset of the behavior is shown in Figure 1. The overall surface motion at this time appears to be a high frequency spray superimposed on a large amplitude low frequency motion in the first antisymmetric slosh mode occurring with rotation. This violent surface agitation entrains air bubbles at various depths under the liquid surface, and, at about 7 g's or more vibrational acceleration, these bubbles do not return to the liquid surface but stream downward to the bottom of the tank. The deeper the bubble is initially thrown from the surface, the more readily it sinks to the container bottom.

As the sinking bubbles reach the container bottom, they begin to coalesce into a cluster which continually grows as more bubbles reach the bottom as shown in Figure 2. Stroboscope observation of the cluster at this time reveals that the entire cluster pulsates at the same frequency as the container motion, and, as the bubble cluster grows, the phase of the bubble pulsation begins to lag behind that of the container. In addition, pressures in the tank bottom also begin to grow in amplitude. This is an accelerating process for more and more bubbles stream downward to the tank bottom.

---

*In addition, a sound motion picture [5] of the preliminary experiments, including slow motion studies, is available.

Suddenly the cluster growth and motion becomes extremely violent as is shown in Figure 3. At this time, the cluster at the bottom pulsates with a very large amplitude while other bubbles rapidly shoot downward from the intensely agitated surface. Pressures in the tank bottom are about 40 psig positive and cavitation pressure negative during this violent pulsation.

After a relatively short period of such violent motion, the whole picture abruptly changes. As can be seen in Figure 4, the entire sequence of the behavior ends as the bubble cluster rises from the tank bottom to a new stable position somewhere in the body of the liquid; the liquid surface, however, continues its violent sloshing. The level to which the cluster rises depends on the vibrational conditions as well as the amount of air entrained in the cluster. The cluster appears to remain at this intermediate level indefinitely, as long as the vibrational conditions are maintained, and as long as more air is not injected into the liquid. Subsequently, raising the frequency, but holding displacement amplitude constant, appears to bring the cluster nearer the surface, while lowering the frequency causes the cluster to seek a lower level in the tank. If the cluster is lowered in this manner, ultimately some critical vibrational conditions are reached at which the cluster can no longer remain submerged, and it vents to the surface. In some cases this is not until the cluster reaches the bottom. As the cluster vents, the violent surface motion ceases.

The entire sequence of events described above takes place in a relatively short time, depending on the vibrational conditions. At 7 g's acceleration and 45 cps frequency, it can occur in as little as 15 seconds with the most violent part of the cluster motion occurring in less than one second. During the entire process, pressure amplitudes in the container bottom were observed to grow as the bubble grows, and were observed to lag more and more behind the container motion, until, during the violent behavior, pressures were very high and lagged the container by about 90°*. After the cluster rose in the liquid, the pressure amplitudes subsided considerably, and their phase with the container motion was between 90° and 180°. This behavior seems to indicate the occurrence of a pressure resonance for constant input conditions.

A pressure probe was used to obtain the pressure distribution at various points in the tank during vibrational conditions less severe than those required to entrain bubbles from surface motion. It was found that in many cases the pressure amplitudes were higher than those predicted for an incompressible fluid in a rigid rank. The pressure distributions were nonlinear with depth, although they were essentially independent of radial position at a given depth. This suggested that the elasticity of the container had to be included in any analysis of the problem since the pressure oscillations in the tank appeared to form a water hammer type

*The pressure forces were so large at this time, in fact, that one of the experimental tanks was ruptured in the course of the tests.

of wave in which the container walls coupled with the liquid. Further, for conditions where bubbles lowered into the liquid, the increase of dynamic pressure with increasing volume of entrained air indicated that the percentage of air in the liquid also affected the velocity of the water hammer wave, as one might have immediately suspected.

The belief that the elasticity of the container and the entrained air in the fluid significantly affected the entire process was further strengthened by additional observations that were made of similar bubble behavior in a 76.2 cm (30 inch) column of water contained in a smaller 6.99 cm (2-3/4 inch) diameter, 0.318 cm (1/8 inch) wall, 99.1 cm (39 inch) high, transparent arcylic plastic tank mounted on an electrodynamic shaker. Higher excitation frequencies could be obtained, but a smaller diameter tank was required because of the much reduced force output of this shaker in comparison to that of the mechanical shaker described previously. In this tank, it was found that a pressure resonance did in fact occur at much lower frequencies that those predicted for water in a rigid tank, even with practically no air in the liquid, and, as air became entrained in the liquid, the resonance could be caused to occur at even lower frequencies.

The entire bubble behavior described above is composed of a large number of individual events, yet the one part which seems to be the most significant is that in which the individual bubbles initially begin to sink to the container bottom, for once this occurs all the rest of the process naturally follows. It is this aspect of the bubble behavior which was

previously investigated by Bleich [2] and for which a theoretical analysis was set forth. The results of this analysis, which are summarized in the next section, were applied to the present tanks in order to predict the acceleration amplitude required to cause small bubbles to sink when injected at a given depth into a vibrating tank of water. For comparison with these predictions, a few preliminary experiments were carried out in the present tanks by injecting small bubbles with a long hypodermic tube. In all cases it was found that considerably less acceleration was required than that predicted by Bleich's theory, assuming the tanks to be rigid and the water as incompressible. Hence, as suggested by the previous preliminary experiments, it was necessary to modify Bleich's theory by allowing for the compressibility of the composite system of liquid, entrained air, and elastic tank.

THEORETICAL ANALYSIS

In his analysis Bleich [2] develops two differential equations which describe the motion of an isolated bubble in a vertically vibrated liquid, and the change in the volume of the bubble caused by the associated pulsating pressure field. They are

$$\ddot{\Delta} + \Omega^2 \Delta = - \frac{\bar{p}}{a\rho} \tag{1}$$

and

$$\frac{\partial}{\partial t} [(a + 3\Delta)\ \dot{z}] = - 2\ (a + 3\Delta) \left(\frac{1}{\rho} \frac{\partial \bar{p}}{\partial z} + g \right) \tag{2}$$

where a is the equilibrium radius of the bubble at a depth z below the surface of an unvibrated liquid; $\bar{p}$ is the dynamic part of the fluid pressure caused by the vibrations, and $\frac{\partial \bar{p}}{\partial z}$ its gradient; Δ is the change in the bubble radius, i. e., the bubble radius at any time is $a + \Delta$; $\Omega = (3\gamma p_1 / \rho a^2)^{1/2}$ is the natural frequency of spherically symmetric pulsations of the bubble [6] in a fluid of density ρ at a depth z where the equilibrium pressure is p_1, and γ is the polytropic constant, equal to 1.4 for adiabatic bubble pulsations and 1.0 for isothermal pulsations. These two coupled equations were originally derived, using energy principles and Lagrange's equations, in a much more complicated nonlinear form than shown here. By using an order of magnitude analysis, Bleich reduced them to the partially linearized form given in Eqs. (1) and (2). Eq. (1) merely states that the variation in the size of the bubble is determined by the variation in

the fluid pressure at the bubble location, and Eq. (2) implies that the instantaneous vertical velocity, $\dot{z}$, of the bubble is determined by its instantaneous bouyancy.

In these equations, it was assumed that the bubble is located in an infinite body of fluid. A more accurate but still approximate calculation taking into account the finite size of the fluid container shows that the first term in Eq. (1) should be multiplied by the factor $(1 + 2ah/R^2)$ where R is the radius of the tank*. However, $2ah/R^2$ is usually not very large compared to unity, and, as will be seen subsequently, the entire first term in Eq. (1) is generally very small compared to the second term; thus, in this analysis Eq. (1) is used as Bleich orginally stated it. Bleich also assumed that the effects of viscosity could be neglected; consequently, Eq. (2) is not valid when the bubble velocity is a sizable fraction of its terminal velocity for a reasonable length of time. It appears, however, that this assumption is very well justified in all of our experiments. A more serious limitation is that the attraction of the pulsating bubble by the free surface and the container walls has been neglected. Hence Eqs. (1) and (2) are good approximations only when the bubble is located in the interior of the fluid. Finally, the effects of the bubble on the fluid pressure in the vicinity of the bubble were also assumed to be very small, and the sloshing of the free surface was neglected.

*This term corrects the "virtual mass" of the bubble pulsations for a finite container. In an unlimited fluid the virtual mass is $2\pi\rho a^3$. The calculations leading to the correction factor are very lengthy, and hence are not reproduced here.

As shown in Figure 5, the tank is vibrated with a motion given by $x_o \cos \omega t$. For this condition, the dynamic pressure in a perfectly rigid tank and for a perfectly incompressible fluid can be expressed as

$$\bar{p} = -\rho z x_o \omega^2 \cos \omega t.$$

Using this formula in Eqs. (1) and (2), and setting the time average of the bouyancy force equal to zero, as shown by Bleich, leads to the result that for a vibrational acceleration amplitude given by

$$\frac{\omega^2 x_o}{g} = \left[2\gamma\left(1 + \frac{p_o}{\rho g h}\right)\right]^{1/2} \tag{3}$$

the bubble is in unstable equilibrium at a depth h. At a slightly greater depth the bubble will sink, at a slightly smaller depth the bubble will rise. Bleich carried out a few experiments in a plastic tank, but he was only able to confirm Eq. (3) qualitatively. As discussed previously, our preliminary experiments also did not check with Eq. (3).

Subsequently, Bleich treated the bubble dynamics in an elastic tank by substituting into Eqs. (1) and (2) the pressure equations he had derived in an earlier paper [7]. His results for this case were quite complicated, and, as a matter of fact, he gave no numerical calculations since he pointed out that his test tank was "rather rigid" because the natural frequency of the ring vibrations* of the tank was much larger than the excitational frequency. He tentatively ascribed the difference between theory and experiment to the effects of viscosity.

*Axially symmetric breathing vibrations.

In the present study the preliminary experiments indicated the presence of pressures greater than those occuring in a rigid tank. By analogy with water hammer waves, we know that it is possible to have large pressure amplifications in longitudinally excited pipes at frequencies considerably smaller than either the natural frequency of the ring vibrations of the pipe or the "organ pipe" frequency of the column of fluid. Hence, a much better correlation of theory and experiment should be possible if the correct fluid pressure in an elastic tank were used in (1) and (2). But the problem of determining these pressures, even for an inviscid fluid, is extremely complex, especially as regards the velocity of propagation of the pressure wave, see, for example, Refs. 8, 9, 10, 11, 12, and 13. Since Eqs. (1) and (2) are themselves somewhat approximate, and since the effects of liquid and structural damping, as well as free surface sloshing, on the pressure wave are very difficult to evaluate, a really complete pressure analysis is not warranted here. A relatively simple approach which still includes the elasticity of the tank is used instead. The method is similar to that used in water hammer analysis, i.e., we assume that the pressure is uniform across any section of the tank, that the deflection of the tank wall is equal to the static deflection caused by the instantaneous fluid pressure, and that longitudinal and bending deflections in the wall can be neglected. For low excitation frequencies, Bleich's results [7] reduce to this condition; the analysis presented here, however, is a good deal simpler than Bleich's and the results are easier to use in numerical calculations.

The first item needed in the analysis is the water hammer wave velocity, or effective speed of sound, for a plane wave propagating axially in the fluid. The usual water hammer wave velocity, however, must be modified to include the effect of the gas dissolved in the liquid since it is possible that considerable quantities of gas bubbles may be present. Hence, let s = ratio of the volume of gas dissolved or entrained in the liquid, usually assumed to be in the form of small bubbles homogeneously distributed throughout the liquid [14, 15], to the total volume of the gas and liquid. Consequently, the mean density of the gas-liquid mixture is

$$\rho = (1-s)\rho_\ell + s\rho_g \tag{4}$$

where ρ_ℓ is the density of the liquid and ρ_g the density of the gas.

The effective compressibility of the gas-liquid-tank system is

$$K = (1-s)\, K_\ell + sK_g + K_t \tag{5}$$

where K_ℓ, K_g, and K_t are the individual compressibilities of the liquid, gas, and tank separately. For an ideal gas, $K_g = (\gamma p)^{-1}$ [16], where p is the gas pressure; p varies with depth in the liquid, but here the variation is neglected and the compressibility is evaluated at the ullage pressure. The compressibility of the tank for this type of wave is $K_t = D/bE$ [17], where D is the tank diameter, b the tank wall thickness, and E the modulus of elasticity of the tank material.

Hence,

$$K = (1 - s)\, K_\ell + \frac{s}{\gamma p_o} + \frac{D}{bE} \tag{6}$$

By definition, the wave velocity is $c = (\rho K)^{-1/2}$ so that

$$c = \left\{\left[(1 - s)\, \rho_\ell + s\rho_g\right]\left[(1 - s)\, K_\ell + \frac{s}{\gamma p_o} + \frac{D}{bE}\right]\right\}^{-1/2} \tag{7}$$

Eq. (7) is shown graphically in Figure 6, for various values of p_o and a typical value of $D/b = 39.0$ for our large experimental tank. It should be noted, however, that Eq. (7) only gives a correct order of magnitude value of the wave velocity, chiefly because the compressibility of the tank is overestimated in Eq. (6); moreover, the exact quantity of gas in the liquid, i. e., the value of s, is difficult to measure experimentally. For these reasons, an experimentally determined wave velocity, measured by a procedure given in the Appendix, is used in all of the numerical calculations. But, Eq. (7) does give a correct qualitative picture, and, as can be seen from Figure 6, quite small values of the speed of sound should be expected.

The fluid pressures can now be determined by treating the pressure wave as a one-dimensional acoustic wave traveling with a velocity c. Thus, if $\xi\,(z, t)$ are the fluid particle displacements measured from their equilibrium positions, then

$$\frac{\partial^2 \xi}{\partial z^2} = \frac{1}{c^2}\, \frac{\partial^2 \xi}{\partial t^2} \tag{8}$$

The boundary conditions require that

$$\xi(\ell, t) = x_o \cos \omega t \tag{9}$$

and

$$\frac{\partial \xi}{\partial z}(0, t) = 0 \tag{10}$$

where Eq. (10) implies that the free surface dynamic pressure is zero. Assuming that

$$\xi(z, t) = f(z) \cos \omega t$$

requires that

$$\xi(z, t) = x_o \frac{\cos \frac{\omega}{c} z}{\cos \frac{\omega}{c} \ell} \cos \omega t \tag{11}$$

in order to satisfy the conditions (9) and (10). Since the pressure is $\rho c^2 \frac{\partial \xi}{\partial z}$ we see that

$$\bar{p}(z, t) = -\rho c \omega x_o \frac{\sin \frac{\omega}{c} z}{\cos \frac{\omega}{c} \ell} \cos \omega t \tag{12}$$

For a rigid tank and imcompressible fluid, $c \to \infty$, and in this case $\bar{p} \to \rho z x_o \omega^2 \cos \omega t$, which checks with Bleich's results for a rigid tank.

Eq. (12) can now be substituted into Eq. (1) to yield

$$\ddot{\Delta}+\Omega^2\Delta = \frac{\omega x_o c}{a} \cdot \frac{\sin \frac{\omega}{c} z}{\cos \frac{\omega}{c} \ell} \cos \omega t \tag{13}$$

or

$$\Delta = \frac{\omega x_o c}{a\Omega^2} \frac{\sin \frac{\omega}{c} z}{\cos \frac{\omega}{c} \ell} \frac{\cos \omega t}{1 - \frac{\omega^2}{\Omega^2}} \tag{14}$$

Since Ω is generally larger than 1,000 cps, the ratio $\frac{\omega^2}{\Omega^2}$ will be neglected in comparison to unity in the subsequent calculations.

The critical value of z, that is, the depth h for bubbles that just start to sink, can be found from Eq. (2) by requiring that the average bouyancy over one cycle of motion be zero, i.e., it must be required that

$$\text{Average of } (a + 3\Delta)\left(\frac{1}{\rho} \frac{\partial \bar{p}}{\partial z} + g\right) = 0 \tag{15}$$

Eq. (15) reduces to

$$ag + \text{Average of } \left[\frac{3\Delta_c}{\rho} \frac{\partial \bar{p}}{\partial z}\right] = 0 \tag{16}$$

where Δ_c is the value of Δ corresponding to the critical value of z.

Solving Eq. (16) gives:

$$2g = \frac{\rho c \omega^3 x_o^2}{\gamma p_1} \frac{\sin \frac{\omega h}{c} \cos \frac{\omega}{c} h}{\cos^2 \left(\frac{\omega}{c} \ell \right)} \tag{17}$$

But $p_1 = p_o + \rho g h$ so that

$$\frac{\omega^2 x_o}{g} \left[\frac{\sin \frac{2\omega h}{c}}{\frac{\omega h}{c} \left(1 + \cos \frac{2\omega \ell}{c} \right)} \right]^{1/2} = \left[2\gamma \left(1 + \frac{p_o}{\rho g h} \right) \right]^{1/2} \tag{18}$$

This equation can be further expressed in terms of nondimensional variables by using the substitutions

$$\phi = \frac{2\omega \ell}{c}, \quad a = \frac{h}{\ell}$$

so that it becomes

$$\left(\frac{\omega^2 x_o}{g} \right) \left[\frac{2 \sin a\phi}{a\phi (1 + \cos \phi)} \right]^{1/2} = \left[2\gamma \left(1 + \frac{1}{a} \frac{p_o}{\rho g \ell} \right) \right]^{1/2} \tag{19}$$

It can be seen that this is a modified form of Eq. (3), the only difference being the factor by which the acceleration is multiplied.* The reciprocal of this factor is shown plotted in Figure 7 for ϕ up to 2π. The full significance of Eq. (19) will be discussed later in connection with the experimental results; here, it is merely pointed out that for $0 < \phi < \pi$ the required acceleration, $\omega^2 x_o$, is always less than that for a perfectly rigid tank.

*It might be pointed out that Eq. (19) can be obtained by substituting our Eq. (12), p. 15, into Eqs. (29) and (33) of Bleich's analysis [2].

Finally, in a rigid tank the motion of the bubble is determined by three parameters: γ, $\frac{\omega^2 x_o}{g}$ and $\frac{p_o}{\rho g h}$. In the elastic tank model analyzed here, however, five parameters are required:

$$\gamma, \frac{\omega^2 x_o}{g}, \frac{2\omega \ell}{c} = \phi, \frac{p_o}{\rho g \ell} \text{ and } \frac{h}{\ell} = \alpha.$$

COMPARISON OF RESULTS

As was mentioned earlier, for an appropriate vertical acceleration amplitude acting on a rigid tank, Bleich's theory predicts that one unstable equilibrium plane will occur at some level h, above which bubbles rise, and below which bubbles sink to the container bottom. When the tank elasticity is included, Bleich predicts that both stable and unstable planes of equilibrium can occur under certain conditions, and that bubbles move away from the unstable planes and collect at the stable planes. It will be seen that for the present case, both of these patterns of behavior will occur under various conditions.

Different patterns of bubble behavior are determined by the variation of the factor

$$\left[\frac{2 \sin a\phi}{a\phi\,(1+\cos\phi)}\right]^{1/2}$$

with both a and ϕ in Eq. (19). For $\phi<\pi$ and any value of a, only one unstable equilibrium plane exists in the tank, so that it acts much like a rigid tank. For $\phi>\pi$ both stable and unstable equilibrium planes can exist in the tank, depending on a. For increasing $\phi>\pi$, the pattern becomes more and more complicated. Of course, for $\phi = n\pi$ where n is an odd integer, a state of pressure resonance exists in the water hammer wave system and very little acceleration (theoretically none) is required to produce the bubble behavior.

Eq. (19) predicts the behavior of small bubbles that are injected into a liquid-air mixture vibrated in an elastic tank. This equation is shown plotted in two different forms in Figures 8 and 9, along with correlating experimental data. These experimental data were obtained from the two different tanks mentioned earlier. In all cases,the data were obtained by injecting small bubbles into the liquids at various levels, while vibrating the tanks under given conditions, and visually observing whether the bubbles moved up or down in the liquid, and whether they sank to the container bottom, or collected at some imtermediate level in the tank. This procedure had to be performed very carefully to avoid giving the bubbles appreciable initial velocities. In addition, the equilibrium levels from which bubbles either moved away or at which they collected were not sharply defined, but rather occupied a narrow band such that bubbles meandered more or less in the vicinity of these bands, and moved rapidly only after leaving them. As a result the exact levels of the equilibrium planes were difficult to determine and some scatter in the data resulted.

For the data of Figures 8 and 9, bubbles were injected into the tanks only after the liquid was swept relatively free of any air bubbles initially present. The speed of water hammer waves for any mixture conditions could be determined using the methods outlined in the Appendix, but it was difficult to maintain a constant amount of air in the water. Therefore in order to obtain consistent results, the tanks were initially swept clear of air bubbles by agitating the tanks under a partial vacuum ullage

pressure prior to taking data. The speed of the water hammer wave for the data was then measured prior to injecting the small bubbles, and the effect of the small amount of injected air on the wave velocity was neglected.

Figure 8 shows a direct plot of Eq. (19) for the two limiting values of $\gamma = 1.0$ and $\gamma = 1.4$. Plotting the curves in this manner, along with the experimental data taken under various conditions, allows one to decide which value of γ most nearly fits the actual process. It can be seen that the data appeared to fit the $\gamma = 1.0$ curve best. As indicated on the plot, the data were taken in both tanks and for various values of all the parameters in the dimensionless number $\frac{1}{a}\frac{P_o}{\rho g \ell}$, except that the acceleration g was necessarily held constant. Water and kerosene were used for two different liquids at various depths, and ullage pressure was changed by subjecting the tank to a partial vacuum.

Figure 9 shows experimental data taken from both tanks using 76.2 cm (30 inches) of water with an ullage pressure of one atmosphere. Here the acceleration required to cause an air bubble to be in equilibrium (stable or unstable) is plotted against the depth ratio, a, each curve for a constant value of ϕ. It may be noted that $\phi = 0$ corresponds to a rigid tank and $\phi = \pi$ corresponds to the first mode pressure resonance of the water hammer wave. For a given ϕ-curve (corresponding to a constant value of $\phi = 2\omega\ell / c$) and a given depth h, a bubble will sink for all acceleration values below the curve. It may be noted that for ϕ less than about 2.0, and for a fixed acceleration input large enough to cause the bubbles to begin to

sink, the bubbles will sink completely to the container bottom. However, for values of ϕ greater, or even somewhat less than π, bubbles injected above a rather shallow depth will rise, but begin to sink if injected at more moderate depths, and eventually collect at a lower, stable depth. Bubbles injected below the lower, stable depth will rise up to this level. As a specific example, consider the $\phi = 4.0$ curve with 6.0 g's acceleration. Bubbles injected above $\alpha = 0.16$ depth ratio will return to the surface, while bubbles injected below this value sink and subsequently collect at a depth value of $\alpha = 0.64$. Bubbles injected below $\alpha = 0.64$ will rise up to that depth value.

The experimental data agree very well with the predicted behavior. All of these data were taken by injecting small bubbles into the tanks and visually observing the levels from which the bubbles moved away in the case of an unstable level and the level at which they collected in the case of a stable one. It may be noted that the liquid depth used was always more than one tank diameter. All values for $\phi = 1.5$ were taken in the large plastic tank. Data for appreciably larger values of ϕ could not be obtained for this tank, as mentioned earlier, because it was necessary to excite the larger tank by means of the frequency limited mechanical shaker. The data for the three values of $\phi > \pi$ were taken in the smaller tank, which could be excited by the electrodynamic shaker. In this range (where the pressure essentially helped drive the shaker), relatively large accelerations could be obtained, but data for $\phi < \pi$ was not obtained since the

acceleration amplitudes at these frequencies were not large enough to cause sinking bubbles. The fact that the tank diameter appears in the theory only as it affects the water hammer wave velocity is supported by these data. However, this is true only as long as the bubbles are small compared to the tank diameter, and probably only for liquid depths greater than one tank diameter.

It has been mentioned that for increasing $\phi > \pi$ the bubble behavior pattern becomes increasingly complicated. This is illustrated in Figure 10 in which the behavior for 76.2 cm (30 inches) of water in the smaller tank is shown for a value of $\phi = 9.75$ and 4 g's acceleration. The equilibrium planes are shown, the upper one being unstable, the second stable, the third unstable, and the fourth stable. Bubble migration directions are indicated by the arrows. Experimental data for such large values of ϕ were not obtained.

EXPLANATION OF OVERALL BUBBLE BEHAVIOR

In view of the preceding analysis and experimental correlations, it is now possible to give a complete explanation of the overall bubble behavior illustrated in Figures 1 through 4. This will be done with the aid of Figure 9.

With very little air initially in the liquid, the wave velocity, c, is 1100 ft/sec (see Appendix). At 7 g's vibrational acceleration and 45 cps ($\phi = 1.29$), bubbles will sink at first only if injected below a depth ratio of about $\alpha = 0.35$ (26.7 cm or 10.5 inches) as can be seen from Figure 9. However, as air bubbles become entrained in the liquid by violent surface motion, the wave velocity immediately begins to decrease (see Figure 6), hence ϕ increases. The more that ϕ increases the more readily the bubbles will sink from near the surface even if the input vibrational conditions are maintained constant. Hence, bubbles begin to sink and a cluster forms and grows at the container bottom where the bubbles collect.

Since an unstable condition exists, the process accelerates until at $\phi = \pi$, corresponding to the first mode pressure resonance in the water hammer wave system, the most violent bubble behavior occurs and dynamic pressures are very large. As a result of the large quantity of air that is entrained in the liquid as the pressure resonance occurs, a value of $\phi > \pi$ ultimately results, the exact value depending on the amount of air entrained, and the whole pattern of bubble behavior changes. According

to Figure 9, if, say, $\phi = 4.5$ results, bubbles can no longer sink below about $\alpha = 0.4$, and the bubble cluster rises from the container bottom to about a depth corresponding to this value of α.

At this point the process becomes stable, for appreciable amounts of air can no longer be entrained from the surface, and, if it could, the further increased value of ϕ would simply cause the cluster to rise slightly nearer the liquid surface. If the frequency is subsequently lowered, holding excitation amplitude constant, both acceleration and ϕ are reduced. The reduced ϕ requires that the cluster be stable at a lower level in the tank, which agrees with experimental observations. Ultimately, the acceleration becomes too small even for ϕ decreasing toward π (since there is damping present) and the cluster can no longer be supported below the surface so that it vents. When this occurs, of course, the system then retains a value of $\phi < \pi$.

In effect, the whole process starts in a system which initially has a pressure resonance at about 110 cps, well above the 45 cps excitation. As the behavior develops, a change in the compressibility of the system occurs, so that the resonant frequency rapidly decreases, passes through the excitation frequency, and ultimately ends up below the excitation frequency. Hence, all of the observed behavior can be explained with the theory developed. However, some quantitative deviation can be expected for at least one important reason--the theory assumes a homogeneous distribution of bubbles, which is not strictly correct during all phases

of the overall behavior. In addition, it is surmised that deviations would exist for liquid levels (ℓ) below one tank diameter, where the assumed pressure distribution would no longer be valid.

Of course, a logical question now arises as to the possible significance of this behavior in an actual space vehicle. One further experiment was performed to help answer this question; the results are shown in Figure 11. The 24.13 cm (9-1/2 inch) diameter tank was fitted with an elliptical plastic bottom having a single 0.19 cm (3/4 inch) drain at the very bottom--a design similar to a number of actual space vehicles. This tank was excited vertically on the mechanical shaker and simultaneously drained. It was found that for conditions where bubbles sank to the tank bottom, a cluster did not form, but all the bubbles immediately surged into the drain pipe--a very serious situation for a space vehicle. The bubbles can readily be seen approaching the drain in Figure 11, although the drain itself cannot be seen because of the cylindrical bottom stiffener.

CONCLUSIONS

The modified Bleich theory appears to be adequate for predicting the observed bubble behavior so long as the assumed conditions exist. In the present experiments, this meant the existence of a system in which a water hammer standing wave could be formed. It is apparent that for a low aspect ratio, more flexible tank, such as those used in space vehicles, the assumptions of plane waves will no longer be adequate. But, the present study indicates that the basic Bleich equations (1) and (2) for bubble behavior can adequately predict bubble behavior in a vibrating liquid providing the proper pressure distribution and gradient for a given tank is incorporated into them. In other words, in order to use these equations to predict bubble behavior, it is obviously imperative that the dynamic pressure field be adequately known for a given tank. Wall effects did not appear to be grossly significant in the present experiments.

Probably the first problem that would arise in a space vehicle because of the bubble behavior reported herein is the passing of the bubbles into the drain pipe and pumping system. In addition, if the entire process occurred, it is apparent that very high dynamic pressures could be experienced in parts of the propellent system, much as has actually been experienced in so called "pogo oscillations" of some vehicles.

If a space vehicle tank subjected to vertical oscillation has a pressure field at all like that of the present tanks, it may readily be seen from

Figure 8 that the lowering of bubbles could occur in a large tank at relatively low acceleration values, even in a fairly rigid tank. Since the composite dimensionless parameter $\frac{1}{4}\frac{p_o}{\rho g \ell}$ could be less than, say, 10.0 for a full size tank, and since most vehicle tanks are relatively flexible, it would appear that bubbles sinking into the drain could be a distinct possibility. An accurate prediction, however, would require that the pressure field of a full size tank be incorporated into Bleich's equations.

ACKNOWLEDGEMENTS

The authors wish to express their sincere appreciation to various members of the Department of Mechanical Sciences for their contributions to the present work. Special mention is extended to Dr. H. N. Abramson for his counsel, to Mr. D. C. Scheidt for assisting in the experimental program, and to Mr. D. M. DeArmond and Mr. V. Hernandez for preparing the figures.

REFERENCES

1. Dodge, F. T., "A Review of Research Studies on Bubble Motion in Liquids Contained in Vertically Vibrating Tanks," Technical Report No. 1, Contract No. NAS8-11045, Southwest Research Institute, December 1963.

2. Bleich, H., "Effect of Vibrations on the Motion of Small Gas Bubbles in a Liquid," Jet Propulsion, 26, Nov. 1956, pp 958-978.

3. Buchanan, R. H., Jameson, G., and Oedjoe, D., "Cyclic Migration of Bubbles in Vertically Vibrating Liquid Columns," Industrial and Engineering Chemistry Fundamentals, 1, No. 2, pp. 82-86.

4. Smith, F. D., "On the Destructive Mechanical Effects of the Gas-Bubbles Liberated by the Passage of Intense Sound Through a Liquid," Philosophical Magazine, Series 7, 19, No. 130, pp. 1147-1151, June 1935.

5. "Bubble Generation and Dynamics in a Vertically Excited Cylindrical Tank" (Motion Picture), Contract No. NAS8-11045, Department of Mechanical Sciences, Southwest Research Institute, San Antonio, Texas.

6. Minnaert, M., "On Musical Air-Bubbles and the Sounds of Running Water," Philosophical Magazine, Series 7, 16, No. 104, August 1933, pp. 235-248.

7. Bleich, H., "Longitudinal Forced Vibrations of Cylindrical Fuel Tanks," Jet Propulsion, 26, February 1956, pp. 109-111.

8. Lamb, H., "On the Velocity of Sound in a Tube, as Affected by the Elasticity of the Walls," Memoirs and Proceedings of the Manchester Literary and Philosophical Society, 42, No. 9, July 1898.

9. Green, H. G., "On the Velocity of Sound in Liquids Contained in Circular Cylinders with Slightly Elastic Walls," Philosophical Magazine, 45, 1923, pp. 907-918.

10. Frederick, D., and King, W. W., "On the Dynamic Response of a Fluid-Filled Cylindrical Shell to an Axially Propagating Pressure Wave, Part III," Virginia Polytechnic Institute, [David Taylor Model Basin, Underwater Explosions Research Division, Contract N189(181) 56489A(X)] February 1964.

11. Skalak, R., "An Extension of the Theory of Water-Hammer," Trans. ASME, 78, 1956, pp. 105-115.

12. Gronwall, T. H., "The Longitudinal Vibrations of a Liquid Contained in a Tube with Elastic Walls," Physical Review, 30, 1927, pp. 71-83.

13. Thomson, W. T., "Transmission of Pressure Waves in Liquid-Filled Tubes," Proc. of 1st U. S. Natl. Cong. of App. Mech., 1951, pp. 927-933.

14. Silberman, E., "Sound Velocity and Attenuation in Bubbly Mixtures Measured in Standing Wave Tubes," J. Acoustical Society of America, 29, No. 8, 1957, pp. 925-933.

15. Chambre, P. L., "Speed of a Plane Wave in a Gross Mixture," J. Acoustical Society of America, 26, No. 3, 1954, pp. 329-331.

16. Lee, J. F., and Sears, F. W., Thermodynamics, Addison-Wesley, 1963.

17. Rich, G. R., Hydraulic Transients, Dover, 1963.

APPENDIX

The water hammer wave velocity, c, had to be determined for use in the parameter $\phi = \frac{2\omega\ell}{c}$, for each tank used to obtain data. Normally this phase velocity is obtained by the classical method of observing experimentally the frequency at which the first mode pressure resonance occurs and then solving for c from a value of $\phi = \pi$. This method actually was used to determine c in the smaller tank, however, it could not be used in the larger tank, since the mechanical shaker could not achieve the frequency at which the first mode pressure resonance occurred when using relatively degassed water in this tank.

A somewhat different method using the pressure distribution as given by equation (12) was utilized. Pressure measurements taken in the smaller tank indicated that equation (12) adequately predicted the pressure distribution for water in that tank at liquid depths well over one tank diameter and for various values of ϕ in the range $0 < \phi < 2\pi$. Therefore, it was assumed that this equation should also adequately predict the pressure distribution in the larger tank under similar depth conditions. Using a pressure probe, pressure distribution data were taken in the larger tank for two different frequencies, each at several different excitation amplitudes. As shown in Figure A-1, these data were then plotted and compared to theoretical curves, each for a constant value of $\phi = \frac{2\omega\ell}{c}$.

The single value of c which made both sets of data best fit the theoretical curves was then taken to be the proper value for the water hammer wave velocity.

Using these methods,it was found that for relatively degassed water in the small tank c = 1380 ft/sec, and for the larger tank c = 1100 ft/sec. Of course these procedures could also be used to determine c for a liquid-air mixture in the tanks, provided that the amount of air in the liquid could be maintained constant,and a method of determining the air volume to total volume ratio was developed.

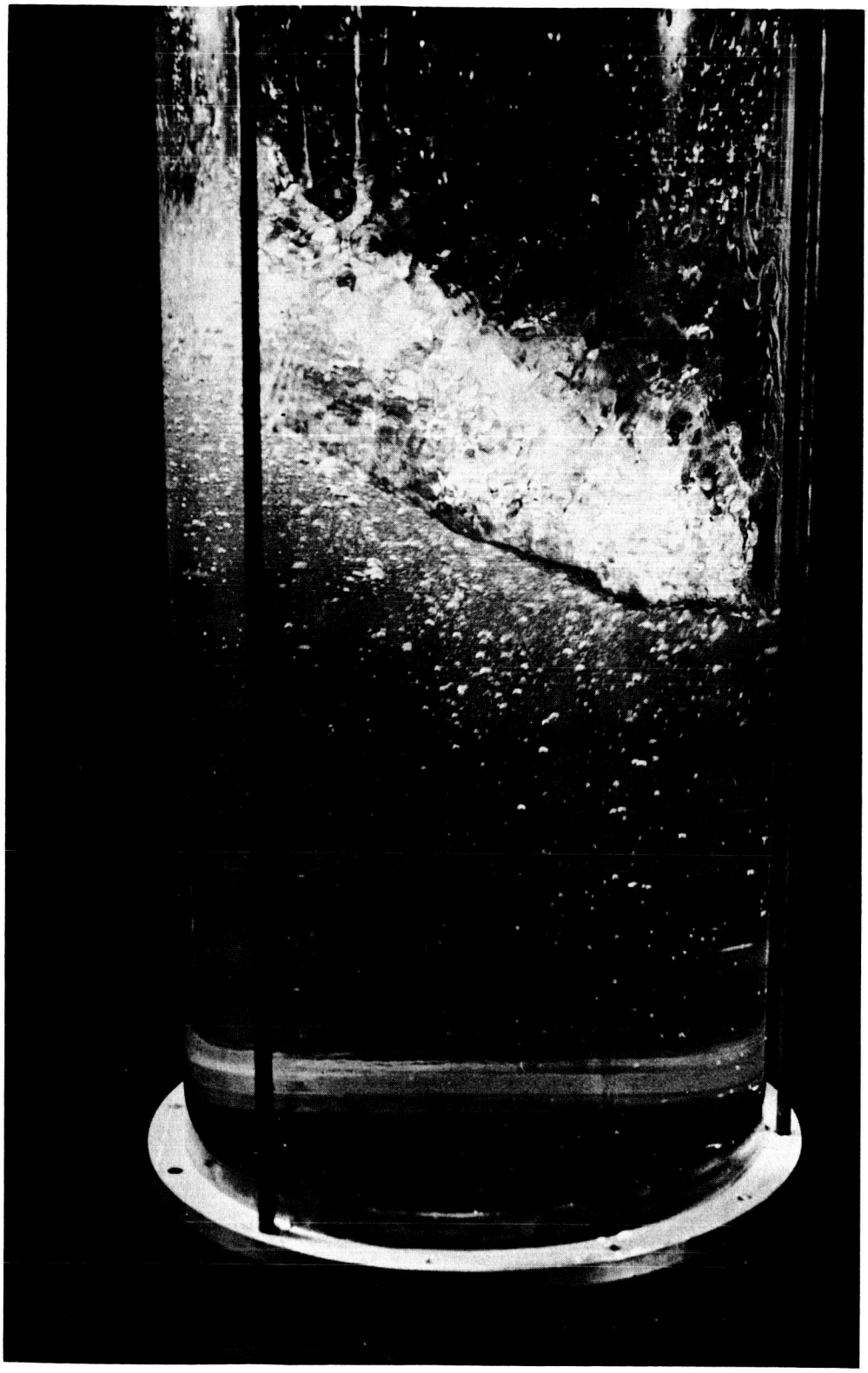

FIGURE 1. ONSET OF BUBBLE BEHAVIOR AT LIQUID SURFACE

FIGURE 2. CLUSTER GROWING AT TANK BOTTOM

FIGURE 3. CLUSTER BEHAVIOR DURING MOST VIOLENT MOTION

FIGURE 4. CLUSTER LOCATION AFTER MOST VIOLENT MOTION

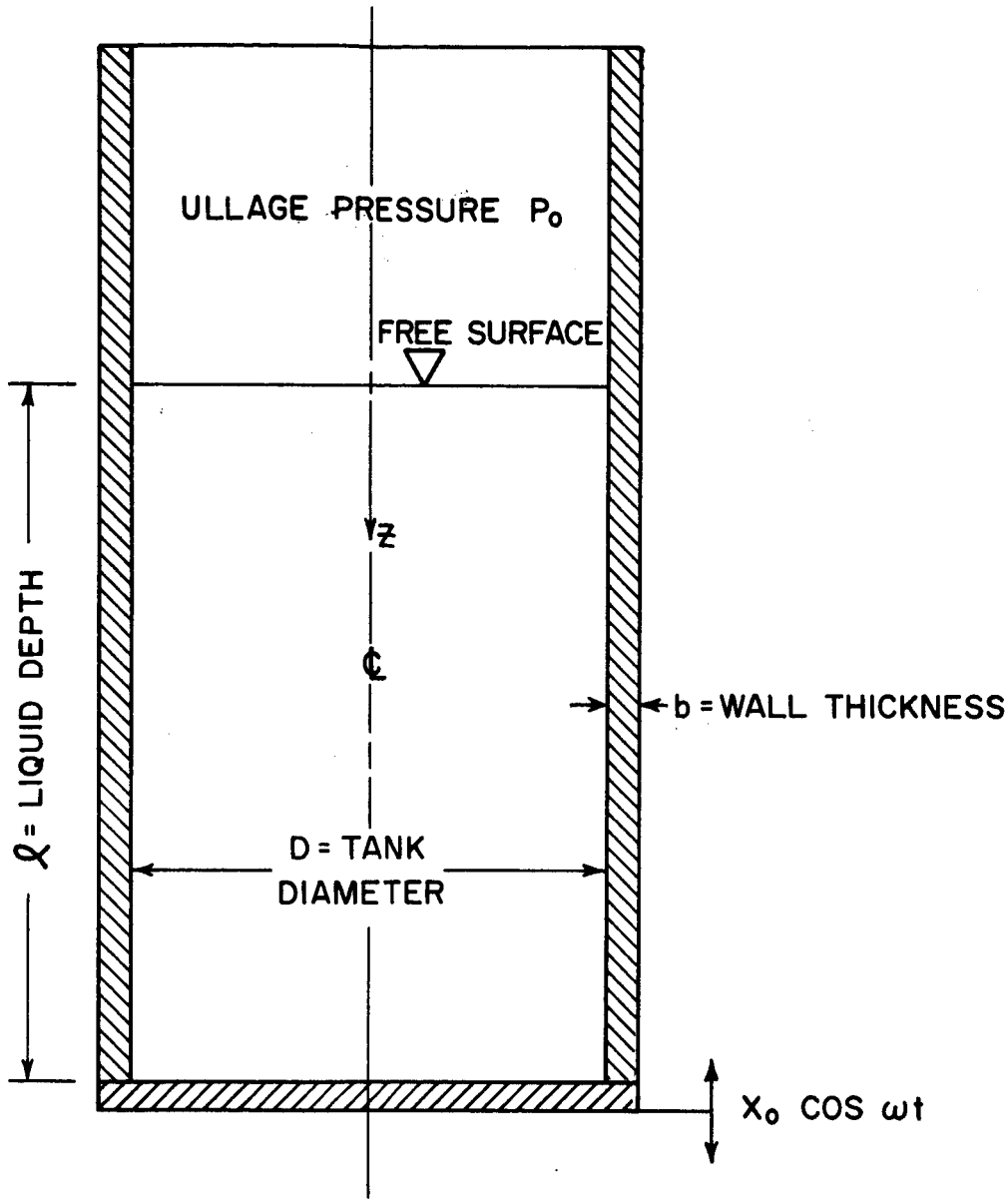

FIGURE 5. CUTAWAY OF CYLINDRICAL TANK WITH COORDINATE SYSTEM

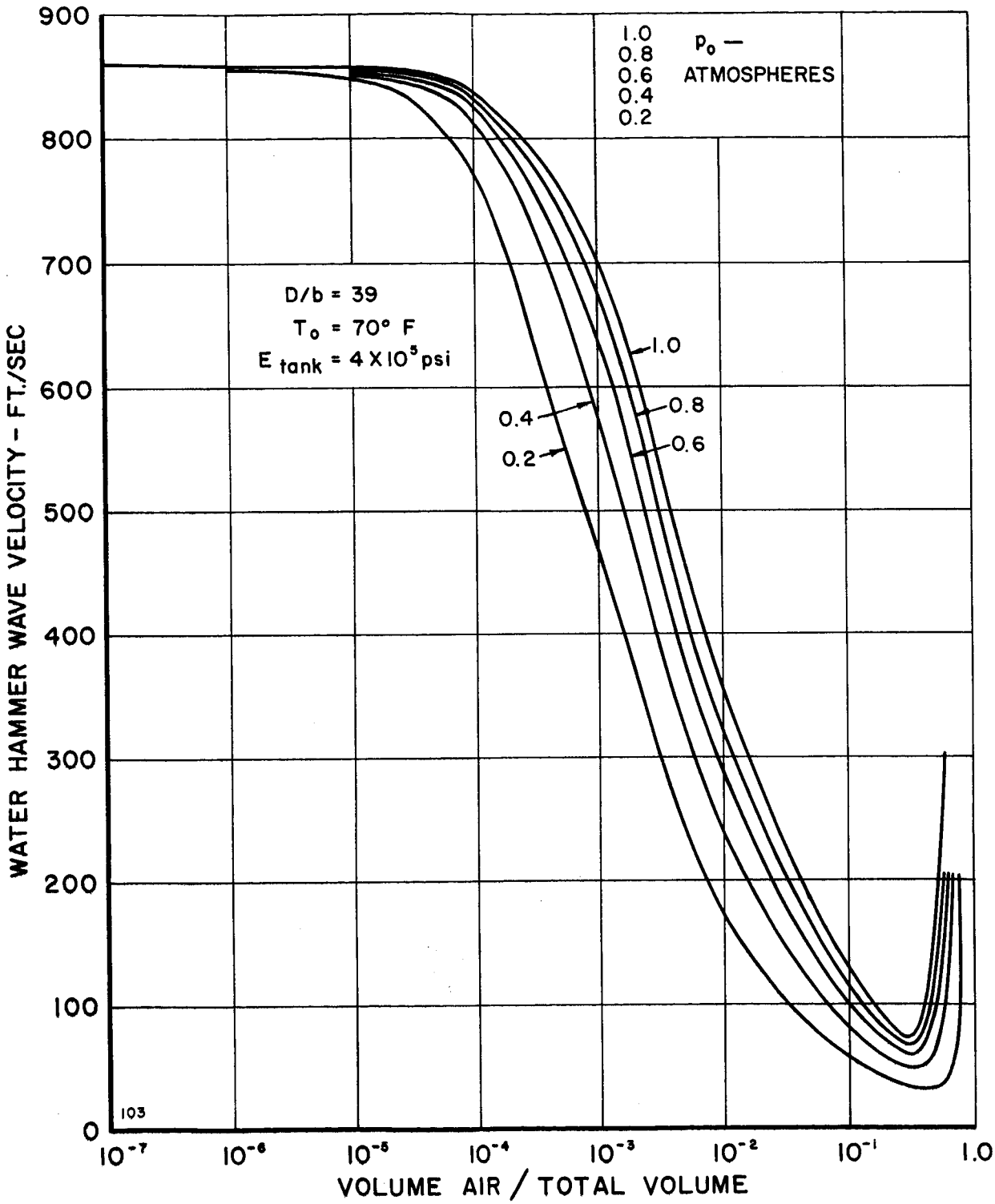

FIGURE 6. WATER HAMMER WAVE VELOCITY IN A LIQUID-AIR MIXTURE

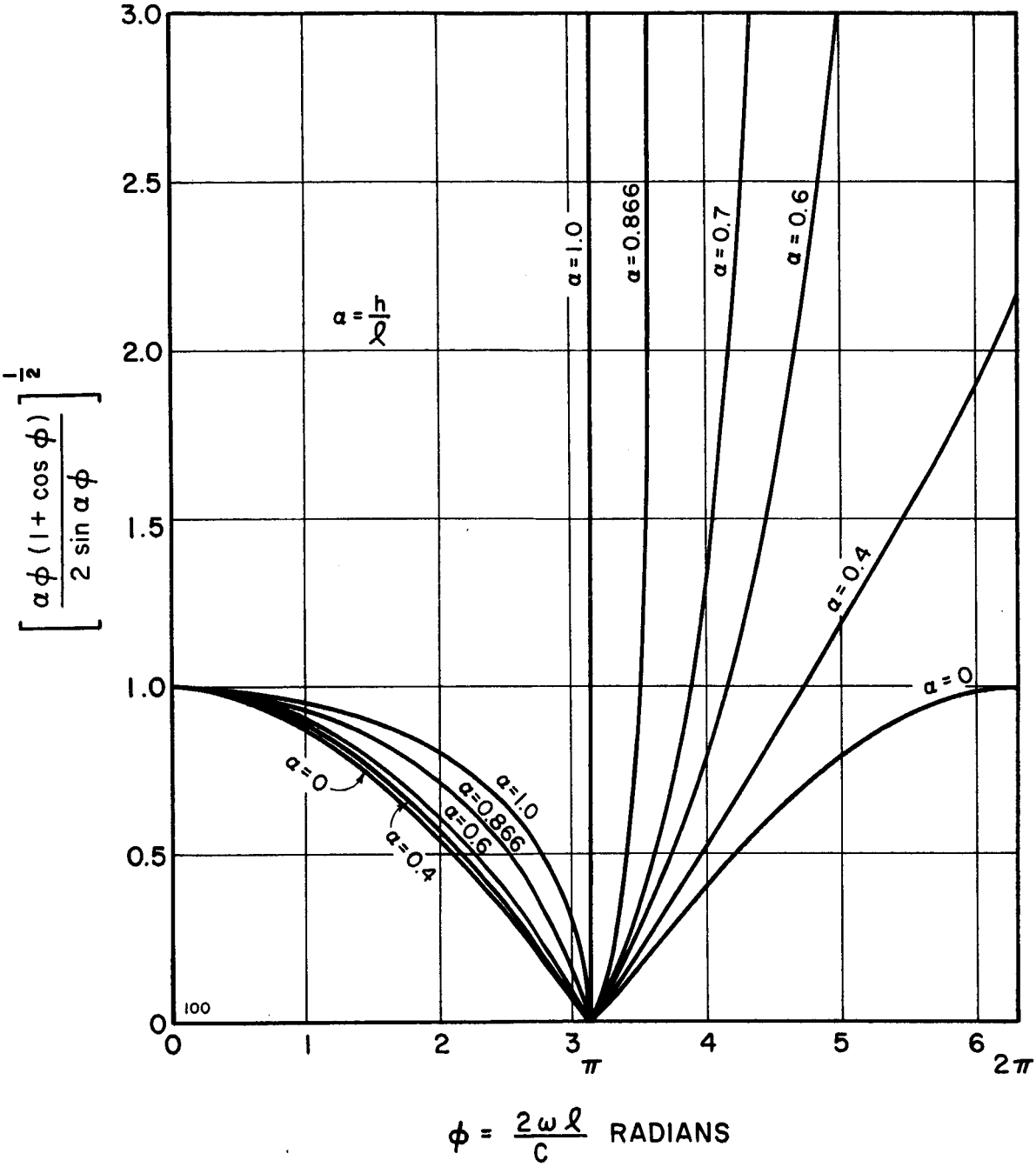

FIGURE 7. VARIATION OF BUBBLE PATTERN FACTOR WITH ϕ

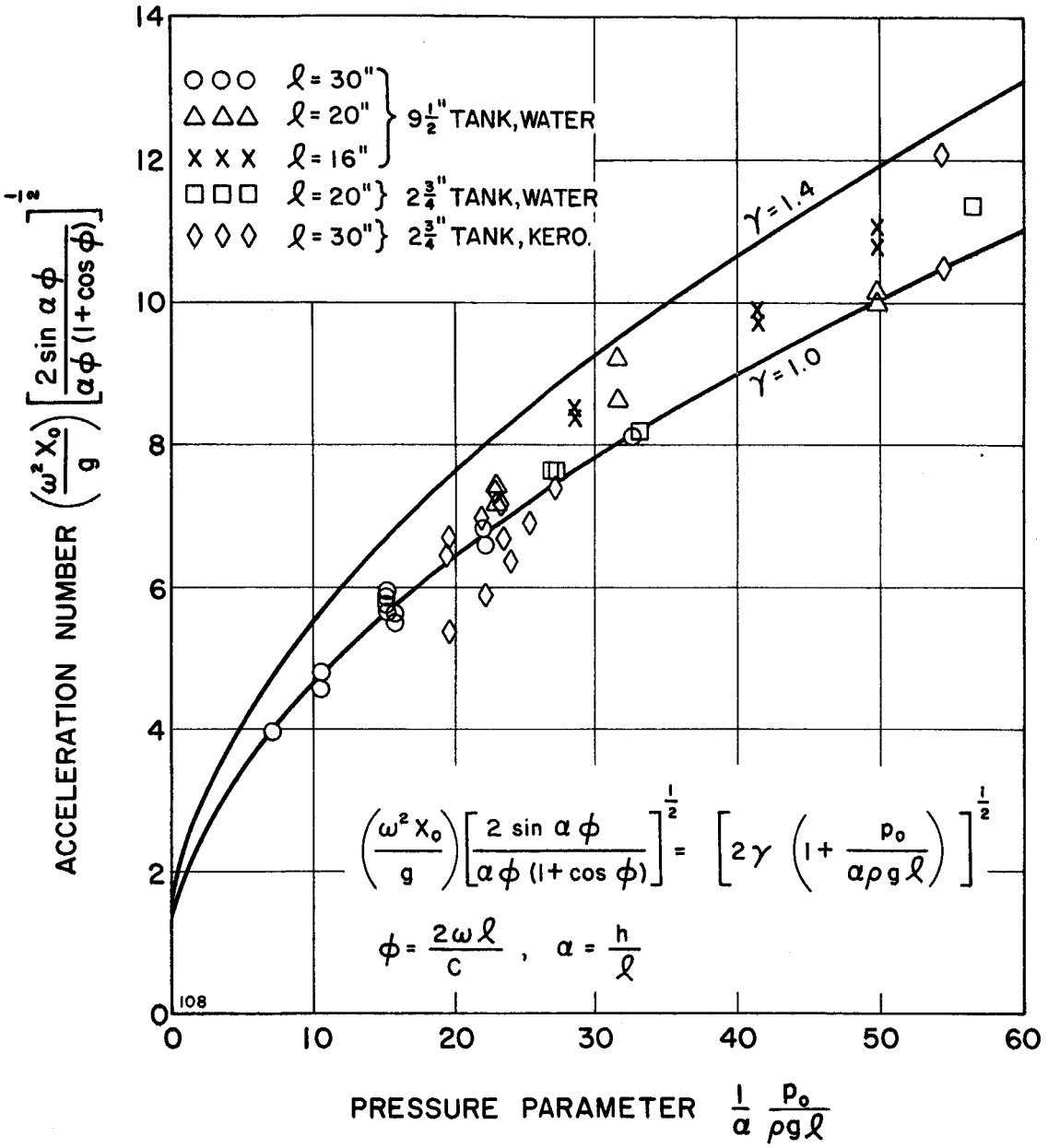

FIGURE 8. VARIATION OF ACCELERATION NUMBER WITH THE COMPOSITE PRESSURE NUMBER

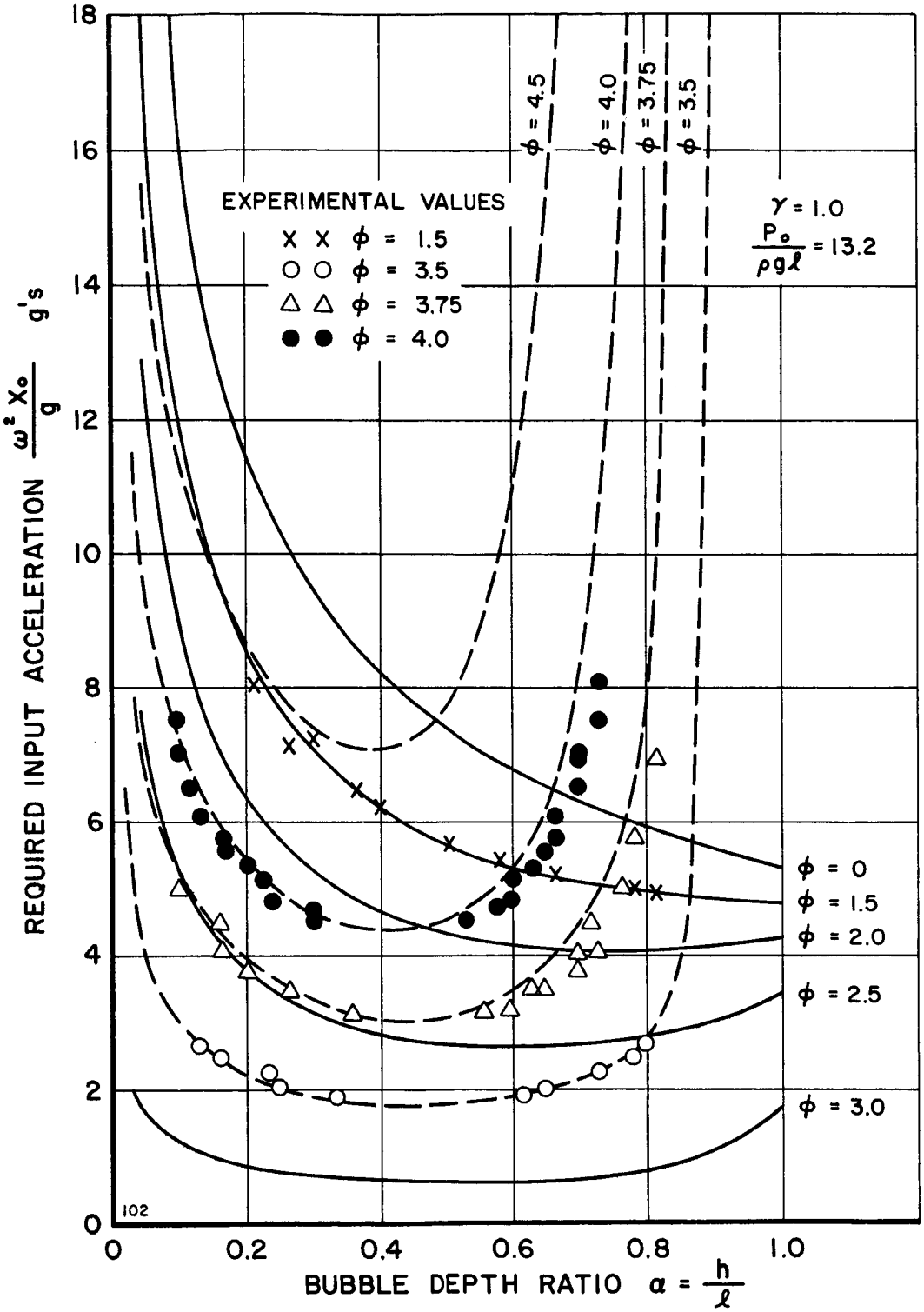

FIGURE 9. VARIATION OF REQUIRED INPUT ACCELERATION WITH DEPTH RATIO

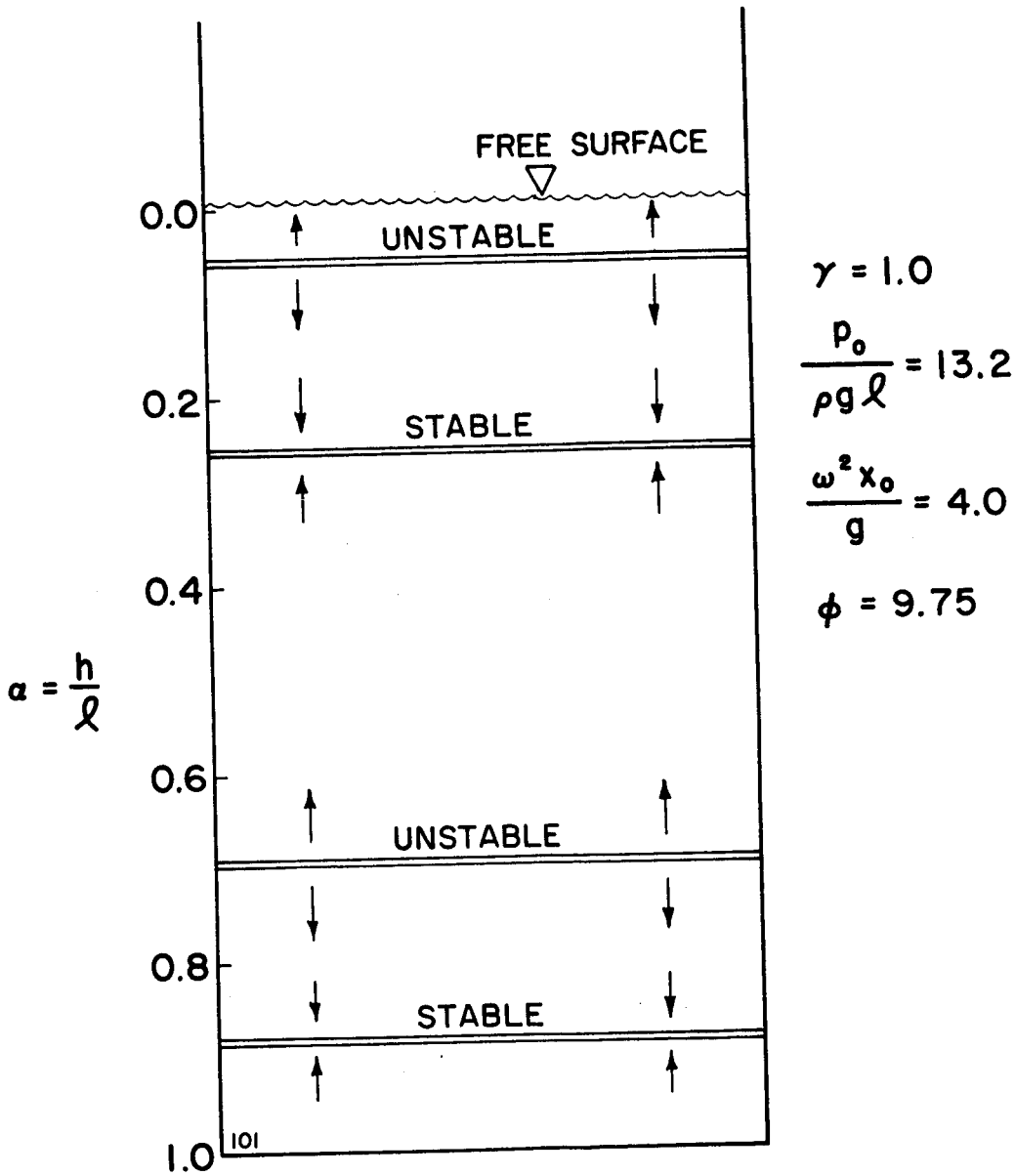

FIGURE 10. BUBBLE PATTERN AT HIGHER FREQUENCY

FIGURE 11. BUBBLES ENTERING DRAIN LINE

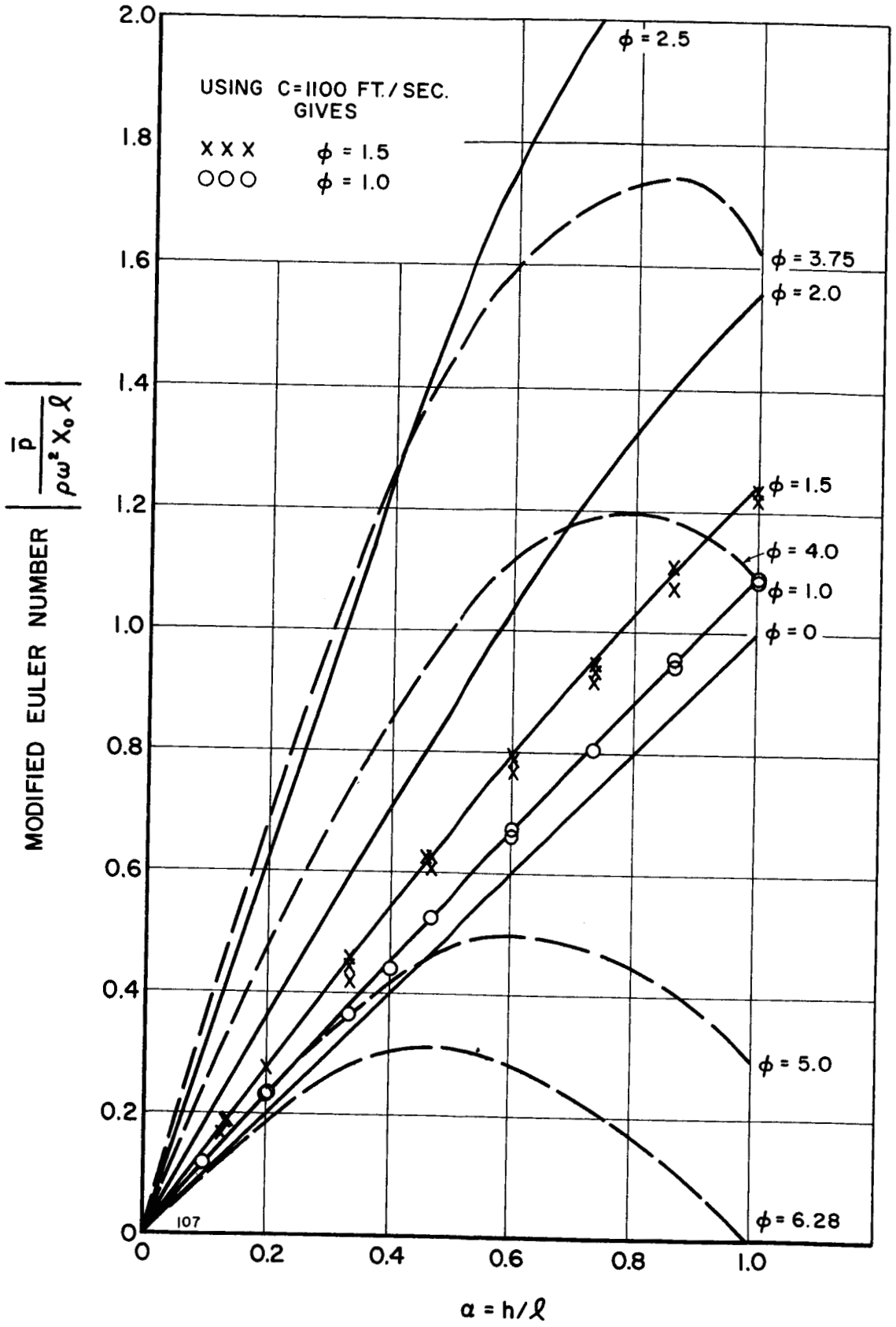

FIGURE A-1. VARIATION OF MODIFIED EULER NUMBER WITH DEPTH RATIO